Stereochemical factors in the transport and binding of photosensitizers in biological systems and in photodynamic therapy

J. W. Winkelman[a], D. Arad[b] and S. Kimel[c,†]

[a]*Brigham and Women's Hospital, Harvard Medical School, Boston, MA 02115 (USA)*
[b]*Department of Microbiology and Biotechnology, Tel Aviv University, Tel Aviv 69978 (Israel)*
[c]*Department of Chemistry, Technion – Israel Institute of Technology, Haifa 32000 (Israel)*

(Received August 26, 1992; accepted January 18, 1993)

Abstract

The uptake and biological activity of porphyrins and phthalocyanines in tumours were correlated with the geometrical features of the photosensitizer molecules. The data suggest that a critical distance of approximately 1.2 nm between oxygen atoms (originating in SO_3^-, COO^- or OH substituents) characterizes a biologically active photosensitizer for photodynamic therapy. We propose that tubulin, which is available in large amounts during mitosis, is the main receptor molecule which binds these photosensitizers. Basic amino acid residues or tightly bound cations in tubulin or homologous proteins may act as binding sites on the receptor molecule.

Keywords: PDT, Sulphonated porphyrins, Phthalocyanines, Tubulin, Modelling of interatomic distances

1. Introduction

Photodynamic therapy (PDT) is an investigational modality for the treatment of cancers. Porphyrin-type photosensitizers are injected and the photochemotherapy of tumours is initiated by the absorption of light at the appropriate wavelength by the tumour-associated photosensitizer [1–3]. PDT is believed to proceed from both intravascular and intracellular events [4].

The sites of action in PDT differ for the various photosensitizers. The lipophilic and oligomeric preparations, such as Photofrin, seem to exert phototoxic effects mainly on endothelial cells, leading to destruction of the tumour vasculature. Hydrophilic and monomeric compounds, such as tetra(4-sulphonatophenyl)porphine) ($TPPS_4$), are believed to target intracellular structures and organelles of the tumour itself [4]. The mechanism by which photosensitizer molecules actually penetrate the cell membrane is largely unknown. Internalization of lipophilic porphyrins seems to be correlated positively to hydrophobicity [5], whereas water-soluble sulphonated porphyrins are known to enter tumour cells *in vivo* and to exert PDT by direct tumour cell effects. This suggests that hydrophilic substances can somehow pass through endothelial cells and vascular membrane structures, diffuse through interstitial spaces and enter tumour and other cells perhaps even more effectively than lipophilic porphyrins and porphyrin analogues. Similar observations have been reported with phthalocyanines [6, 7].

In the past decade intensive research has been carried out to correlate the biological activity of photosensitizers with their chemical constitution [8–10]. In a more systematic approach, series of increasingly sulphonated porphyrins and metallophthalocyanines have been synthesized and their biological activity determined. Biological activity *in vitro* pertains to cellular uptake and retention of a photosensitizer and to cellular photoinactivation; *in vivo* studies involve transport and distribution of a photosensitizer in tissue and photodynamically induced regression of a tumour.

The photosensitizers considered here include *meso*-tetraphenylporphine with n peripheral sulphonate substituents at the para positions ($n = 1$, 2, 3 or 4) ($TPPS_n$), various coordinated metal-ion phthalocyanines with n sulphonate substituents on the macrocycle ($MPcS_n$) (M ≡ Al, Ga, Zn) and *meso*-tetrahydroxyphenylporphine (THPP). The physicochemical properties of these compounds

†Author to whom correspondence should be addressed.

1011-1344/93/$6.00

TABLE 1. Relative values of biological activity of $TPPS_n$ *in vitro*

$TPPS_n$	Cellular uptake			Cellular photoinactivation		
	[12]	[14]	[28]	[12]	[14]	[28]
$TPPS_1$	7.6	22.7	1.1[a], 1.0[b]	8.6	3.9	24
$TPPS_{2a}$	15.0	27.0	0.9[a], 1.3[b]	26.7	3.4	22
$TPPS_{2o}$	5.0	11.0	0.5[a], 0.7[b]	10.6	1.8	0.8
$TPPS_3$	1.5	–	–, –	2.7	–	–
$TPPS_4$	1.0	1.0	1.5[a], 1.7[b]	1.0	1.0	1.0

[a]Light-induced intracellular relocalization.
[b]As footnote a after trypsinization.

vary considerably. They range from lipophilic (when $n=0$ or 1) to hydrophilic (when $n=3$ or 4). The disulphonated porphyrins ($n=2$) consist of two isomers: amphiphilic $TPPS_{2a}$ (with two SO_3^- groups on adjacent phenyl rings) and hydrophilic $TPPS_{2o}$ (with two SO_3^- groups on opposite phenyl rings). Similarly, we distinguish between PcS_{2a} and PcS_{2o} with two sulphonate substituents on adjacent and opposite phthalic subunits respectively.

There is evidence that the degree of sulphonation and the specific geometry of related porphyrins have a major effect on cellular uptake and on binding to particular intracellular targets. The earliest report on the distribution of $TPPS_4$ in animal tumour systems showed it to be associated with the cytosolic fraction of the tumour cells and to confer its characteristic red fluorescence diffusely in the cytoplasm of the tumour and other cells [11]. The amphiphilic compound $TPPS_{2a}$ is taken up by cells in culture to a greater extent than $TPPS_{2o}$ or other $TPPS_n$ compounds [12–14]. For $MPcS_2$, a similar configurational feature has been reported for biological activity *in vitro* [15–22] and in experimental tumours *in vivo* [16, 17, 22–25]. Finally, large differences in biological activity have been reported for the positional isomers *o*-THPP, *m*-THPP and *p*-THPP [26, 27].

Tables 1 and 2 present the biological activity *in vitro* of sulphonated porphyrins and phthalocyanines respectively. Table 3 presents the biological activity *in vivo* of $MPcS_n$ compounds. All entries are relative to the value reported for the corresponding tetrasulphonated compound. The tabulated material clearly shows that adjacently substituted disulphonated compounds manifest singular biological activity compared with all the other sulphonated photosensitizers. This conclusion, which is based on the extensive data collected in Tables 1–3, can be extended to biochemical interactions which occur without light, since it has been found that $TPPS_{2a}$ binds more strongly to the tubulin subunits of microtubules compared with $TPPS_{2o}$ or other $TPPS_n$ compounds with $n=3$ or 4 [29, 30].

The marked difference in the relative efficiency of uptake of disulphonated photosensitizers prompted us to look for structure–activity relationships. Consequently, we studied the geometrical features of the following: (i) the adjacent and opposite isomers of $TPPS_2$ and $MPcS_2$; (ii) THPP with one hydroxyl group at the ortho, meta or para position on each of the phenyls; (iii) dihaematoporphyrin ether/ester (DHE), one of the photoactive constituents of Photofrin; (iv) bis(8-anilino-naphthalene-1-sulphonate) (bis-ANS), a known disulphonated tubulin-binding agent [31]. We searched for common structural characteristics which may determine the behaviour in biological systems.

The results reported here suggest that polar substituents (whether SO_3^-, COO^- or OH), spaced approximately 1.2 nm apart, are a common stereochemical feature which may foster cellular uptake and intracellular binding of photosensitizers, particularly binding to tubulin. In tumours and other rapidly dividing cells, tubulin is available in larger amounts since microtubule assembly and disassembly are characteristically very high during mitosis [32, 33]. Thus enhanced binding to tubulin

TABLE 2. Relative values of biological activity of $MPcS_n$ *in vitro*

$MPcS_n$	Cellular uptake		Cellular photoinactivation				
	[19] M≡Al	[22] M≡Al	[15] M≡Ga	[16] M≡Zn	[18] M≡Al	[20] M≡Al	[21] M≡Al
$MPcS_1$	10.2	22	–	14.3[b]	–	2.2	2.2
$MPcS_2$	3.6	7.0	40 (280[a])	36.7	22	3.1	2.1
$MPcS_3$	1.3	0.8	5	6.1	8.5	1.3	–
$MPcS_4$	1.0	1.0	1.0	1.0	1.0	1.0	1.0

[a]Activity of the pure (4,4′) isomer of $GaPcS_{2a}$.
[b]$n=1.6$.

TABLE 3. Relative values of biological activity of $MPcS_n$ *in vivo*

$MPcS_n$	Tumour uptake			Tumour regression		
	[22] M≡Al	[23] M≡Al	[24] M≡Al/Zn	[16] M≡Zn	[23] M≡Al	[24] M≡Al/Zn
$MPcS_1$	<0.01	–	–	2.5	–	–
$MPcS_2$	0.2	0.4	1.5/2.4	9.8	1.5	1.2/2.5
$MPcS_3$	0.7	–	–	0.9	–	–
$MPcS_4$	1.0	1.0	1.0/1.0	1.0	1.0	1.0/1.0

may help to explain the preferential intracellular uptake of these photosensitizers by tumours. This fundamental mechanism of uptake and binding should be considered in addition to the ionic [9, 10] and lipophilic or amphiphilic character of photosensitizer molecules [10].

2. Methods

Structural modelling was carried out with an SGI-20G work station (Silicon Graphics, Inc., Mountain View, CA) using QUANTA software (Polygen Corporation, Waltham, MA). The atomic coordinates of TPP and of the phthalocyanine macrocycle were imported from the Cambridge Crystallographic Data Base (CCDB); experimental data [34, 35] were used. Free-base porphyrins can crystallize either in a planar conformation [34] or in a saddle conformation [36]. This indicates that the interconversion energy is relatively low so that the porphyrin molecule in solution will adapt itself to the relevant geometry of the receptor site. For phthalocyanines, deviations from planarity are even less pronounced [35]. Both skeletons retrieved from CCDB were planar.

The model structure for $TPPS_4$ (Fig. 1, see Section 3) was obtained by attaching sulphonate groups (SO_3^-) to the para positions in the aromatic rings. This substitution does not affect the geometry of the TPP skeleton, as was confirmed by semi-empirical (AM1) quantum mechanical calculations [37] on the *p*-(methylvinyl)benzene sulphonate building block of TPP. The peripheral sulphonate groups are free to rotate around the C–S bond so that each O^- is situated on the base of a cone. For any two SO_3^- groups in the macrocycle this gives rise to different O^-–O^- distances ranging from $(O^-–O^-)_{min}$ to $(O^-–O^-)_{max}$.

In PcS_{2o} (Fig. 2, see Section 3) there is a possibility of forming two constitutional isomers (SO_3^- groups located at 4,4′ or 4,5′ positions of the two phthalic subunits), whereas in PcS_{2a} there

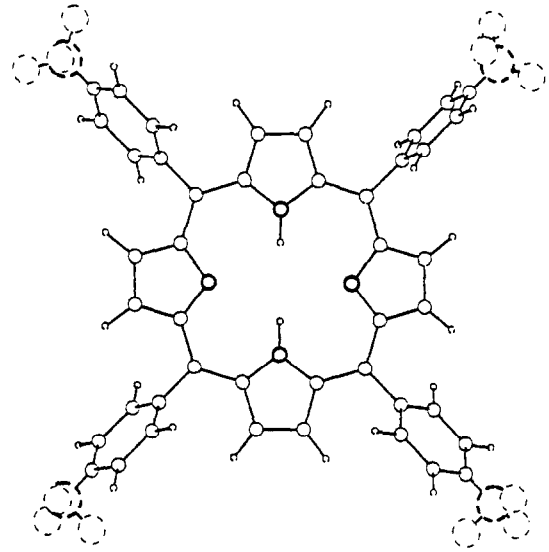

Fig. 1. Model structure of $TPPS_4$ (scale, 50 mm nm^{-1}). The compound *p*-THPP is obtained by replacing the SO_3^- groups by OH.

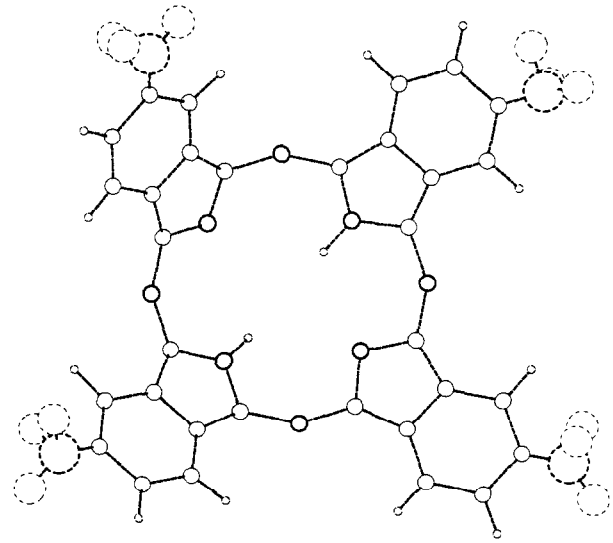

Fig. 2. Model structure of PcS_4 (scale, 50 mm nm^{-1}).

TABLE 4. Non-bonded energy contributions (kJ mol^{-1}) of DHE (ether) from molecular mechanics calculations; constant angle $\phi = 94°$ and varying angle ψ

ψ (°)	Energy	
	Lennard–Jones	Electrostatic
0	1.8×10^{4}	49
25	2×10^{4}	70
50	2×10^{6}	65
60	1.9×10^{4}	68
74	1.8×10^{4}	45
84	5.1×10^{2}	24
94	1×10^{3}	32
104	2.4×10^{4}	54
114	2×10^{6}	57
124	1.8×10^{4}	50
134	1.8×10^{4}	48
145	9×10^{9}	59
160	2×10^{8}	58

are three isomers (4,4′, 4,5′ or 5,4′ positions), where we have adopted the numbering convention used by van Lier [7]. For each isomer there is a range of O^-–O^- distances due to rotation of the sulphonate groups.

For *p*-THPP the O–O distance between two hydroxyls on different phenyls is accurately defined. For *o*-THPP and *m*-THPP the O–O distance depends on the torsion angle θ between the plane of the phenyl ring and that of the macrocycle (due to steric hindrance $\theta = 90° \pm 5°$ for *o*-THPP and $\theta = 90° \pm 30°$ for *m*-THPP).

For Photofrin we consider DHE, one of the photoactive constituents believed to be effective in PDT. The two porphyrin moieties of the DHE skeleton are connected by an ether or an ester bond [38]. The total energy as a function of rotation of the two moieties around the connecting bond was calculated using the molecular mechanics program CHARMM [39]. Analysis of the contributions of the electrostatic and the steric plus non-bonded van der Waals' energies (based on the Lennard–Jones potential) shows that the steric energy contribution is dominant. For the ether (see Table 4), the barrier for rotation is high due to steric hindrance between the two methyl groups adjacent to the link (Fig. 3, see Section 3). Only distinct conformations can exist (torsional angles around the ether bonds $\phi = 94°$ and $\psi = 84°$, see Fig. 3) with the methyl groups in the trans orientation. For the ester, the two porphyrin moieties are relatively free to rotate with respect to the planar configuration, within the limits of the torsional angles around the ester bonds, $45° < \phi < 105°$ and $0° < \psi < 60°$. Beyond these angles, unfavourable steric interactions between the two porphyrin macrocycles sharply increase the calculated molecular mechanics energy of the system. Distances between O^- of the anionic groups COO^-, situated on the two moieties of DHE, were calculated for the energetically preferred configurations of the ether and the ester form.

3. Results

Figures 1 and 2 show the $TPPS_4$ and PcS_4 structures. Figure 3 presents the DHE molecule with an ether link between the two moieties. The molecule is depicted as a stereoscopic pair, in the energetically most favourable configuration with respect to torsion around the ether link. Figure 4 shows the bis-ANS molecule.

Figure 5 shows the modelled distances between the positions of O^- in SO_3^- groups (in $TPPS_2$, PcS_2 and bis-ANS) and of O^- situated in COO^- (in DHE). For each case we present, as needed, values of $(O^-\text{–}O^-)_{min}$ and $(O^-\text{–}O^-)_{max}$. It should be noted that, for porphyrins, these distances will be different if the macrocycle is in the saddle conformation. The O^-–O^- distances on adjacent rings will increase by up to 15%, while on opposite rings they will decrease by 20%. However, these conformational variations will not affect our conclusion (Fig. 5) that the preferred distance in the tumour or in the tubulin receptors can be matched

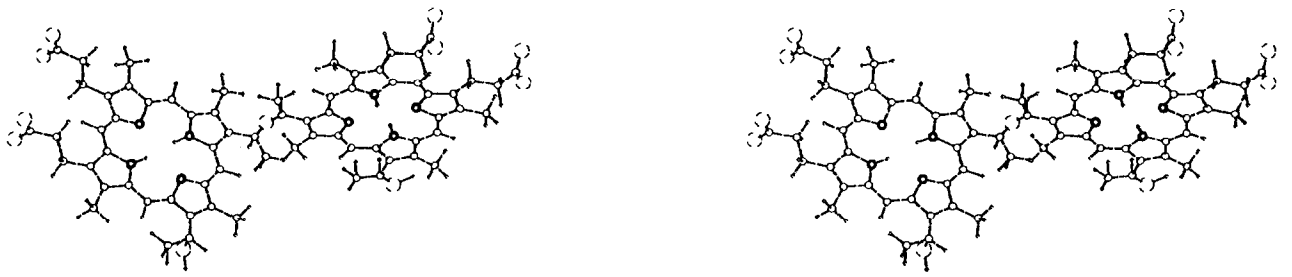

Fig. 3. Model structure of DHE in a stereoscopic representation (scale, 25 mm nm^{-1}).

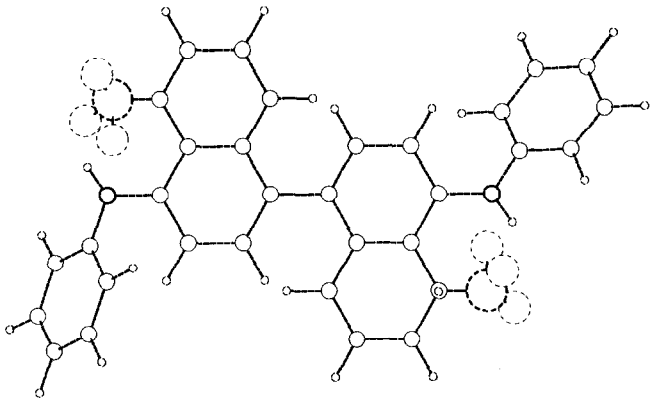

Fig. 4. Model structure of bis-ANS (scale, 50 mm nm^{-1}).

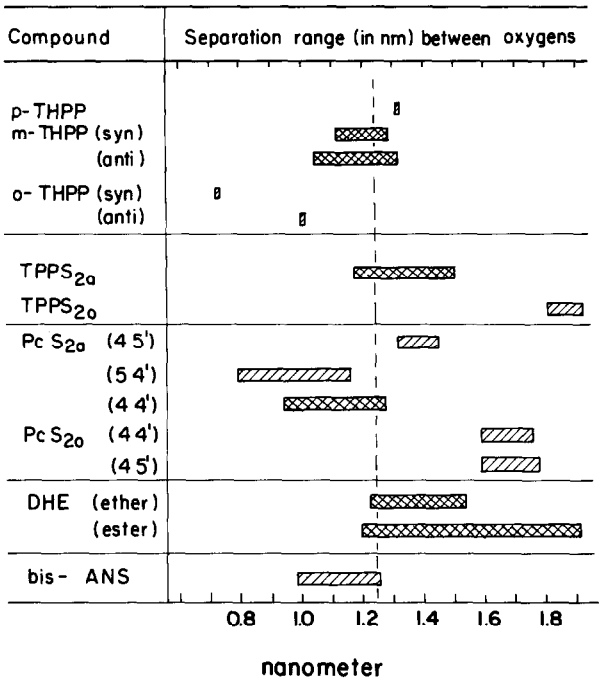

Fig. 5. Scalar representation of O–O distances of selected active (▩) and inactive (▨) dye molecules.

only by compounds with polar substituents on adjacent rings. In any case, several structures coexist in solution and the configuration of the porphyrin molecule will adapt itself to fit the receptor site. Figure 5 also depicts the O–O distances between two adjacent hydroxyls in the positional isomers of THPP [26, 27], where we have taken into account the possibility of the existence of the syn configuration ($\theta_1 = \theta_2$) and the anti configuration ($\theta_1 = \theta_2 + 180°$) for *o*-THPP and *m*-THPP.

4. Discussion

Porphyrins and related compounds that have been considered as potential agents for PDT must ultimately exert their effects at the molecular level. Conventional pharmacological research seeks to relate chemical structure to function by focusing on the specific biochemical mechanism that is enhanced or inhibited. This often involves the modification of candidate pharmaceutical molecules, once the molecular target is known, so that the structure–activity relationship is optimized. In the field of PDT, this approach has thus far been largely neglected and structure–activity relationships have been determined empirically.

4.1. Uptake in vitro

Numerous factors influence the cellular uptake in culture of porphyrins and phthalocyanines; one is the degree of sulphonation (Tables 1 and 2). Increasing the number of sulphonate groups in PcS_n decreases the lipid–water partition coefficient [18] and correlates inversely with PcS_n uptake. This decrease in uptake is presumably due to the less favoured diffusion of higher sulphonated derivatives through lipid cell membranes. The hydrophobicity argument, by itself, may perhaps explain the preferred uptake of lipophilic, less-sulphonated phthalocyanine derivatives. However, it cannot explain the results for $TPPS_n$, since $TPPS_{2a}$ uptake is larger than that of $TPPS_1$; nor can it account for the different uptake of $TPPS_n$ compared with that of PcS_n having equivalent hydrophobicity. Finally, a large difference in photoinactivation has been reported [15] for the three constitutional isomers of $GaPcS_{2a}$ which possess similar amphiphilic character.

4.2. Intracellular distribution

The binding of porphyrins to specific intracellular targets at the molecular rather than the organelle level may help to understand the distribution, the photoinduced action in PDT and the toxic effect in the dark. A specific intracellular binder with high affinity, even for a minority constituent of a porphyrin preparation, could therefore be of considerable interest. Such binding could act as a "diffusion sink" and change the kinetics of accumulation in cells. It could also focus attention on biochemical effects attributable to perturbation of the normal function of the target molecules. For example, binding to tubulin can influence the uptake and distribution *in vitro* and *in vivo* since the dynamic equilibrium is shifted towards the movement of extracellular porphyrin into the cytoplasm. Furthermore, specific binding to tubulin could explain several known biological effects of $TPPS_n$, including mitotic arrest in metaphase, inhibition of microtubule assembly *in vitro* [29, 30],

light-induced redistribution inside cells [28, 40, 41] and dark toxicity *in vivo* [42].

The intracellular transport and localization of $TPPS_n$ and PcS_n [28, 41] are also dependent on the number and position of the SO_3^- groups (Tables 1–3). $TPPS_{2a}$ has been shown to redistribute among intracellular compartments, after low-level light exposures, with subsequent increased phototoxicity [28], consistent with prior observations of greater photoinactivation from intracellular *vs.* membrane-bound $TPPS_n$ [14].

4.3. Uptake in vivo

Data on the PDT efficacy in whole animal systems as a function of the degree of sulphonation of photosensitizers are scarce (see Table 3). The pharmacokinetics of these compounds *in vivo* is further confounded by effects of the route of administration, by encapsulation in lipoproteins or artificial micellar vehicles, by vascular *vs.* stromal *vs.* intracellular ingress and egress and by differences in the mixture of cells within various target organs [4, 22, 43–45].

Contrary to findings *in vitro*, the uptake of sulphonated $TPPS_n$ [12] and PcS_n [16, 17, 22–25] *in vivo* does not correlate positively with hydrophobicity. Indeed, Chan *et al.* [22] have reported a negative correlation with hydrophobicity of $AlPcS_n$.

4.4. Possible binding sites and binding modes in tubulin

There is evidence that monomeric or heterodimeric tubulin is the target for $TPPS_4$ photodamage. This favoured target constitutes approximately half of the total intracellular tubulin, which is in dynamic equilibrium with microtubules [33]. Mitotic inhibition in metaphase of human cell lines *in vitro* by porphyrins and phthalocyanines has recently been shown to be due to perturbation of the microtubules in the mitotic spindle [30, 46–49]. One mechanism proposed for damage to the spindle from photoactivated $TPPS_n$ is from a primary effect on the tubulin monomer. Depolymerization of microtubules by nocodazole prior to light exposure of $TPPS_4$-loaded NHIK 3025 cells further inhibits microtubule repolymerization and increases the number of cells arrested in metaphase [47].

The amino acid sequences of α and β tubulin have been determined [50, 51], but the tertiary structure is still unknown. Cationic binding sites at the stereochemically required distance may be provided by amino acids with net positive charge. A cluster of basic residues in tubulin is composed of Arg-390, His-393 and Lys-394 (Arg, arginine; His, histidine; Lys, lysine). Microtubule assembly has been shown to be highly dependent on the region around this cluster [52]. We suggest that this region is an excellent candidate binding site for $TPPS_n$.

An alternative binding site may be provided by tightly bound cations. From energy transfer studies the binding of the potent inhibitor of microtubule assembly, bis-ANS [31], to tubulin was shown to be localized in the C-terminal domain [53], which is different from the binding of other anti-mitotic tubulin-binding drugs, such as colchicine. Since bis-ANS is a disulphonated compound it is reasonable to assume that the disulphonated molecules $TPPS_{2a}$ and PcS_{2a} (in which the SO_3^- groups are separated by the same distance as in bis-ANS) bind to the same site in tubulin. The C-terminal domain in tubulin contains two Ca^{2+}-binding sites, one in the sequence region between residues 407 and 427 and the other between residues 423 and 446 [54, 55].

The Ca^{2+}-binding regions in tubulin show sequence homology to the corresponding regions in the Ca-binding proteins calmodulin and troponin-C [55], the three-dimensional structures of which have been determined [56, 57]. The coordinates of these proteins are available from the "Protein Data Bank" [58]. Both proteins contain four Ca^{2+}-binding sites: two exposed sites in the C-terminal region and two less exposed sites in the N-terminal region. By inspecting the three-dimensional structures of both proteins it was observed that the distance between the two exposed Ca^{2+} ions is 1.18 nm in calmodulin and 1.17 nm in troponin-C [58]. The arrangement around the exposed Ca^{2+} ions is a square bipyramid, the six ligands being oxygens of the side-chain residues aspartic and glutamic acid or serine and of the carbonyl backbone. Sometimes an external ligand is replaced by a water molecule.

It is tempting to hypothesize that the three-dimensional structure of tubulin, in the C-terminal region, is similar to that of calmodulin and troponin. We suggest that the two SO_3^- groups in bis-ANS bind to the Ca^{2+} ions of tubulin by replacing an external ligand in a topographically favoured orientation. Similarly, it is suggested that an SO_3^- group (of $TPPS_n$ or PcS_n), a CO_2^- group (DHE) or a hydroxyl group (THPP) can replace an external ligand at the exposed Ca^{2+} site of tubulin. The binding of photosensitizers to biomolecules also depends on π interactions. However, at the present time these cannot be quantified since the site and the three-dimensional structure of the receptor

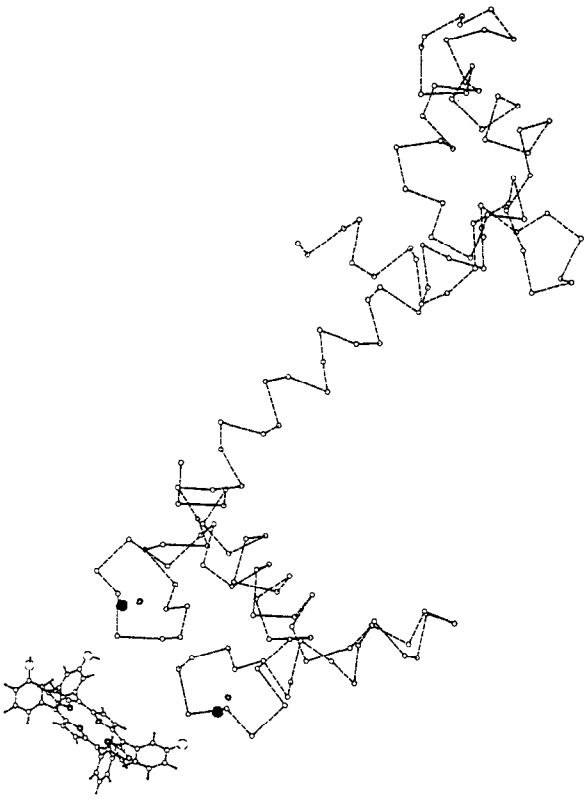

Fig. 6. Hypothetical model structure of an *m*-THPP molecule bound to a calmodulin skeleton (scale, 15 mm nm^{-1}): ●, Ca^{2+} ions.

molecule are not known. Instead, we specified the electrostatic interactions, as derived from the structure–activity relationships, as a first step towards a complete determination. The hypothesized structure of *m*-THPP bound to calmodulin (as an example of receptor molecules of this type) is shown in Fig. 6.

It is pleasing to note that the distances between the polar groups of the more active dipolar compounds in PDT are all around 1.2 nm (see Fig. 5), *i.e.* very close to the distance between the external ligands that bind to the two exposed Ca^{2+} ions. The hypothesis presented in this paper can be verified experimentally by investigating the binding of specific $TPPS_n$, PcS_n and THPP molecules to calmodulin or troponin. This work is now in progress.

Acknowledgments

This research was supported in part by grant 88-00308 of the US–Israel Binational Science Foundation, Jerusalem, and by the Fund for the Promotion of Research at the Technion.

References

1 B. W. Henderson and T. J. Dougherty, How does photodynamic therapy work? *Photochem. Photobiol., 55* (1992) 145–157.
2 C. N. Zhou, Mechanisms of tumor necrosis induced by photodynamic therapy, *J. Photochem. Photobiol. B: Biol., 3* (1989) 299–318.
3 D. Kessel (ed.), *Photodynamic Therapy of Neoplastic Disease,* Vols. 1 and 2, CRC Press, Boca Raton, FL, 1990.
4 J. W. Winkelman and S. Kimel, The relationship between porphyrin transport and tissue uptake with photosensitization from $^1O_2$, in D. Kessel (ed.), *Photodynamic Therapy of Neoplastic Disease,* Vol. 2, CRC Press, Boca Raton, FL, 1990, pp. 29–42.
5 D. Kessel, Transport and binding of hematoporphyrin derivative and related porphyrins by murine leukemia L 1210 cells, *Cancer Res., 41* (1981) 1318–1323.
6 E. Ben-Hur, M. Green, A. Prager, R. Kol and I. Rosenthal, Phthalocyanine photosensitization of mammalian cells: biochemical and ultrastructural effects, *Photochem. Photobiol., 46* (1987) 651–656.
7 J. E. van Lier, Phthalocyanines as sensitizers for PDT of cancer, in D. Kessel (ed.), *Photodynamic Therapy of Neoplastic Disease,* Vol. 1, CRC Press, Boca Raton, FL, 1990, pp. 279–290.
8 J. Moan, Q. Peng, J. F. Evensen, K. Berg, A. Western and C. Rimington, Photosensitizing efficiencies, tumor- and cellular uptake of different photosensitizing drugs relevant for photodynamic therapy of cancer, *Photochem. Photobiol., 46* (1987) 713–721.
9 R. Pottier and J. C. Kennedy, The possible role of ionic species in selective biodistribution of photochemotherapeutic agents toward neoplastic tissue, *J. Photochem. Photobiol. B: Biol., 8* (1990) 1–16.
10 D. Brault, Physical chemistry of porphyrins and their interactions with membranes: the importance of pH, *J. Photochem. Photobiol., B: Biol., 6* (1990) 79–86.
11 J. W. Winkelman and S. Spicer, Staining with tetraphenylporphine-sulfonate *in vivo, Stain Technol., 37* (1962) 303–305.
12 D. Kessel, P. Thompson, K. Saatio and K. D. Nantwi, Tumor localization and photosensitization by sulfonated derivatives of tetraphenylporphine, *Photochem. Photobiol., 45* (1987) 787–790.
13 K. Berg, A. Western, J. C. Bommer and J. Moan, Intracellular localization of sulfonated meso-tetraphenylporphines in a human carcinoma cell line, *Photochem. Photobiol., 52* (1990) 481–487.
14 K. Berg, J. C. Bommer, J. W. Winkelman and J. Moan, Cellular uptake and relative efficiency in cell inactivation by photoactivated sulfonated *meso*-tetraphenylporphines, *Photochem. Photobiol., 52* (1990) 775–781.
15 N. Brasseur, H. Ali, R. Langlois and J. E. van Lier, Biological activities of phthalocyanines – VII. Photoinactivation of V-79 Chinese hamster cells by selectively sulfonated gallium phthalocyanines, *Photochem. Photobiol., 46* (1987) 739–744.
16 N. Brasseur, H. Ali, R. Langlois and J. E. van Lier, Biological activities of phthalocyanines – IX. Photosensitization of V-79 Chinese hamster cells and EMT-6 mouse mammary tumor by selectively sulfonated zinc phthalocyanines, *Photochem. Photobiol., 47* (1988) 705–711.
17 J. Rousseau, R. Langlois, H. Ali and J. E. van Lier, Biological activities of phthalocyanines XII: synthesis, tumor uptake and biodistribution of ^{14}C-labeled disulfonated and trisulfonated gallium phthalocyanine in C3H mice, *J. Photochem. Photobiol. B: Biol., 6* (1990) 121–132.

18 B. Paquette, H. Ali, R. Langlois and J. E. van Lier, Biological activities of phthalocyanines – VIII. Cellular distribution in V-79 Chinese hamster cells and phototoxicity of selectively sulfonated aluminum phthalocyanines, *Photochem. Photobiol., 47* (1988) 215–220.

19 K. Berg, J. C. Bommer and J. Moan, Evaluation of sulphonated aluminum phthalocyanines for use in photochemotherapy. Cellular uptake studies, *Cancer Lett., 44* (1989) 7–15.

20 K. Berg, J. C. Bommer and J. Moan, Evaluation of sulfonated aluminum phthalocyanines for use in photochemotherapy. A study on the relative efficiencies of photoinactivation, *Photochem. Photobiol., 49* (1989) 587–594.

21 J. Moan, K. Berg, J. C. Bommer and A. Western, Action spectra of phthalocyanines with respect to photosensitization of cells, *Photochem. Photobiol., 56* (1992) 171–175.

22 W.-S. Chan, J. F. Marshall, R. Svensen, J. Bedwell and I. R. Hart, Effect of sulfonation on the cell and tissue distribution of the photosensitizer aluminum phthalocyanine, *Cancer Res., 50* (1990) 4533–4538.

23 P. T. Chatlani, J. Bedwell, A. J. MacRobert, H. Barr, P. B. Boulos, N. Krasner, D. Phillips and S. G. Bown, Comparison of distribution and photodynamic effects of di- and tetrasulphonated aluminium phthalocyanines in normal rat colon, *Photochem. Photobiol., 53* (1991) 745–751.

24 H. L. L. M. van Leengoed, N. van der Veen, A. A. C. Versteeg, A. E. van der Berg-Blok, J. P. A. Marijnissen and W. M. Star, Tumour tissue imaging using the localizing properties and fluorescence of some phthalocyanines, *Int. J. Radiat. Biol., 60* (1991) 121–124.

25 Q. Peng, J. Moan, J. M. Nesland and C. Rimington, Aluminum phthalocyanines with asymmetrical lower sulfonation and with symmetrical higher sulfonation: a comparison of localizing and photosensitizing mechanism in human tumor LOX xenografts, *Int. J. Cancer, 46* (1990) 719–726.

26 M. Berenbaum and R. Bonnett, *Meso*-tetra(hydroxyphenyl) porphyrins, in D. Kessel (ed.), *Photodynamic Therapy of Neoplastic Disease,* Vol. 2, CRC Press, Boca Raton, FL, 1990, pp. 169–177.

27 Q. Peng, J. Moan, J. M. Nesland, J. F. Evensen, M. Kongshaug and C. Rimington, Localizing and photosensitizing mechanism by tetra(3-hydroxyphenyl) porphine *in vivo* on human malignant melanoma xenografts in athymic nude mice, *Lasers Med. Sci., 5* (1990) 399–409.

28 K. Berg, K. Madslien, J. C. Bommer, R. Oftebro, J. W. Winkelman and J. Moan, Light induced relocalization of sulfonated *meso*-tetraphenylporphines in NHIK 3025 cells and effects of dose fractionation, *Photochem. Photobiol., 53* (1991) 203–210.

29 K. Boekelheide, J. Eveleth, A. H. Tatum and J. W. Winkelman, Microtubule assembly inhibition by porphyrins and related compounds, *Photochem. Photobiol., 46* (1987) 657–661.

30 K. Berg, J. Moan, J. C. Bommer and J. W. Winkelman, Cellular inhibition of microtubule assembly by photoactivated sulphonated *meso*-tetraphenylporphines, *Int. J. Radiat. Biol., 58* (1990) 475–487.

31 P. Horowitz, V. Prasad and R. F. Luduena, Bis(1,8-anilinonaphthalenesulfonate): a novel and potent inhibitor of microtubule assembly, *J. Biol. Chem., 259* (1984) 14 647–14 650.

32 W. M. Saxton, D. L. Stemple, R. J. Leslie, E. D. Salmon, M. Zavortink and J. R. McIntosh, Tubulin dynamics in cultured mammalian cells, *J. Cell Biol., 99* (1984) 2175–2186.

33 J. Avila, Microtubule dynamics, *FASEB J., 4* (1990) 3284–3290.

34 R. J. Butcher, G. B. Jameson and C. B. Storm, Crystal structure of *meso*-tetratolylporphyrin: implications for the solid-state ^{15}N CPMAS NMR, *J. Am. Chem. Soc., 107* (1985) 2978–2980.

35 D. Dolphin (ed.), *The Porphyrins,* Vol. III, Academic Press, New York, 1978, pp. 463–529.

36 M. J. Hamor, T. A. Hamor and J. L. Hoard, The structure of crystalline tetraphenylporphine. The stereochemical nature of the porphine skeleton, *J. Am. Chem. Soc., 86* (1964) 1938–1942.

37 M. J. S. Dewar, E. G. Zoebisch, E. F. Healy and J. J. P. Stewart, AM1: a new general purpose quantum mechanical molecular model, *J. Am. Chem. Soc., 107* (1985) 3902–3909.

38 D. Kessel, Proposed structure of the tumor-localizing fraction of HPD (hematoporphyrin derivative), *Photochem. Photobiol., 44* (1986) 193–196.

39 B. R. Brooks, R. E. Bruccoleri, B. D. Olafson, D. I. States, S. Swaminathan and M. Karplus, CHARMM: a program for macromolecular energy minimization and dynamics calculations, *J. Comput. Chem., 4* (1983) 187–217.

40 A. Rück, T. Köllner, A. Dietrich, W. Strauss and H. Schneckenburger, Fluorescence formation during photodynamic therapy in the nucleus of cells incubated with cationic and anionic water-soluble photosensitizers, *J. Photochem. Photobiol. B: Biol., 12* (1992) 403–412.

41 Q. Peng, G. W. Farranto, K. Madslien, J. C. Bommer, J. Moan, J. E. Danielsen and J. M. Nesland, Subcellular localization, redistribution and photobleaching of sulfonated aluminum phthalocyanines in a human melanoma cell line, *Int. J. Cancer, 49* (1991) 290–295.

42 J. W. Winkelman and G. H. Collins, Neurotoxicity of tetraphenylporphine sulfonate $TPPS_4$ and its relation to photodynamic therapy, *Photochem. Photobiol., 46* (1987) 801–807.

43 M. Kongshaug, J. Moan and S. B. Brown, The distribution of porphyrins with different tumour localising ability among human plasma proteins, *Br. J. Cancer, 59* (1989) 184–188.

44 G. Jori and E. Reddi, Strategies for tumor targeting by photodynamic sensitizers, in D. Kessel (ed.), *Photodynamic Therapy of Neoplastic Disease,* Vol. 2, CRC Press, Boca Raton, FL, 1990, pp. 117–130.

45 C. Milanesi, C. Zhou, R. Biolo and G. Jori, Zn(II) phthalocyanine as a photodynamic agent for tumours. II. Studies on the mechanism of photosensitized tumour necrosis, *Br. J. Cancer, 61* (1990) 846–850.

46 L. A. Sporn and T. H. Foster, Photofrin and light induces microtubule depolymerization in cultured human endothelial cells, *Cancer Res., 52* (1992) 3443–3448.

47 K. Berg, H. B. Steen, J. W. Winkelman and J. Moan, Synergistic effects of photoactivated tetra(4-sulfonatophenyl) porphine and nocodazole on microtubule assembly, accumulation of cells in mitosis and cell survival, *J. Photochem. Photobiol. B: Biol., 13* (1992) 59–70.

48 K. Berg, The unpolymerized form of tubulin is the target for microtubule inhibition by photoactivated tetra(4-sulfonatophenyl)porphine, *Biochem. Biophys. Acta, Mol. Cell Res., 1135* (1992) 147–153.

49 K. Berg and J. Moan, Mitotic inhibition by phenylporphines and tetrasulfonated aluminium phthalocyanine in combination with light, *Photochem. Photobiol., 56* (1992) 333–339.

50 H. Ponstingl, E. Krauhs, M. Little and T. Kempf, Complete amino acid sequence of α-tubulin from porcine brain, *Proc. Natl. Acad. Sci. USA, 78* (1981) 2757–2761.

51 E. Krauhs, M. Little, T. Kempf, R. Hofer-Warbinck, W. Ade and H. Ponstingl, Complete amino acid sequence of β-tubulin from porcine brain, *Proc. Natl. Acad. Sci. USA, 78* (1981) 4156–4160.

52 J. Szasz, M. B. Yaffe, M. Elzinga, G. S. Blank and H. Sternlicht, Microtubule assembly is dependent on a cluster of basic residues in α-tubulin, *Biochemistry, 25* (1986) 4572–4582.
53 A. R. S. Prasad, R. F. Luduena and P. M. Horowitz, Detection of energy transfer between tryptophan residues in the tubulin molecule and bound bis(8-anilinonaphthalene-1-sulfonate), an inhibitor of microtubule assembly, that binds to a flexible region on tubulin, *Biochemistry, 25* (1986) 3536–3540.
54 R. B. Maccioni, L. Serrano and J. Avila, Structural and functional domains of tubulin, *BioEssays, 2* (1985) 165–169.
55 L. Serrano, A. Valencia, R. Caballero and J. Avila, Localization of the high affinity calcium-binding site on the tubulin molecule, *J. Biol. Chem., 261* (1986) 7076–7081.
56 Y. S. Babu, J. S. Sack, T. J. Greenhough, C. E. Bugg, A. R. Means and W. J. Cook, Three-dimensional structure of calmodulin, *Nature, 315* (1985) 37–40.
57 O. Herzberg and M. N. G. James, Refined crystal structure of troponin C from turkey skeletal muscle at 2.0 angstroms resolution, *J. Mol. Biol., 203* (1988) 761–768.
58 Brookhaven National Laboratory, *"Protein Data Bank"*, 1991.